Equilibrium and nonequilibrium entanglement properties of 2D and 3D Fermi gases

Jacopo Nespolo and Ettore Vicari
Dipartimento di Fisica dell'Università di Pisa and INFN, Pisa, Italy

We investigate the entanglement properties of the equilibrium and nonequilibrium quantum dynamics of 2D and 3D Fermi gases, by computing entanglement entropies of extended space regions, which generally show multiplicative logarithmic corrections to the leading power-law behaviors, corresponding to the logarithmic corrections to the area law.

We consider 2D and 3D Fermi gases of N particles constrained within a limited space region, for example by a hard-wall trap, at equilibrium at $T = 0$, i.e. in their ground state, and compute the first few terms of the asymptotic large-N behaviors of entanglement entropies and particle fluctuations of subsystems with some convenient geometries, which allow us to significantly extend their computation. Then, we consider their nonequilibrium dynamics after instantaneously dropping the hard-wall trap, which allows the gas to expand freely. We compute the time dependence of the von Neumann entanglement entropy of space regions around the original trap. We show that at small time it is characterized by the relation $S \approx \pi^2 V/3$ with the particle variance, and multiplicative logarithmic corrections to the leading power law, i.e. $S \sim t^{1-d} \ln(1/t)$.

PACS numbers: 03.65.Ud,05.30.Fk,67.85.-d

I. INTRODUCTION

The nature of the quantum correlations of many-body systems, and in particular the entanglement phenomenon, are fundamental physical issues. They have attracted much theoretical interest in the last few decades, due to the progress in the experimental activity in atomic physics, quantum optics and nanoscience, which has provided a great opportunity to investigate the interplay between quantum and statistical behaviors in particle systems. In particular, the great ability in the manipulation of cold atoms [1–3] allows the realization of physical systems which are accurately described by theoretical models, such as dilute atomic Fermi and Bose gases, Hubbard and Bose-Hubbard models, with different effective spatial dimensions from one to three, achieving thorough experimental checks of the fundamental paradigma of the condensed matter physics. Experiments with cold atoms allow to investigate the unitary quantum evolution of closed many-body systems, exploiting their low dissipation rate which maintains phase coherence for a long time [3, 4]. In this experimental context, the theoretical investigation of nonequilibrium dynamics in quantum many-body systems, and the time evolution of the entanglement properties characterizing the quantum correlations, is of great importance for a deep understanding of the fundamental issues of quantum dynamics, their possible applications, and new developments.

Quantum correlations are characterized by the fundamental phenomenon of entanglement, which gives rise to nontrivial connections between different parts of extended quantum systems [5–7]. A measure of entanglement is provided by the entanglement entropies associated with the reduced density matrix $\rho_A = \mathrm{Tr}_B \rho$ of a subsystem A with respect to its complement B. The entanglement properties of 1D systems have been substantially understood, and in particular a leading logarithmic behavior has been established at conformally invariant quantum critical points [8]. However, in higher dimensions the scaling behavior of the bipartite entanglement entropy is generally more complicated, without a definite general scenario for the universal behavior at a quantum phase transition.

In general, the entanglement entropy is asymptotically proportional to the surface separating the two subsystems A and B. The area law has been generally proven for gapped systems [9], independently of the statistics of the microscopical constituents. On the other hand, lattice free fermions show multiplicative logarithmic corrections to the area law [10–18]. Indeed, for a large subsystem A of size l_A the entanglement entropy scales as

$$S_A^{(\alpha)} \sim l_A^{d-1} \ln l_A, \tag{1}$$

where $S^{(\alpha)}$ are the Rényi entropies defined as

$$S_A^{(\alpha)} = \frac{1}{1-\alpha} \ln \mathrm{Tr} \rho_A^\alpha, \tag{2}$$

whose limit $\alpha \to 1$ gives the von Neumann (vN) entropy

$$S_A^{(1)} = -\mathrm{Tr} \rho_A \ln \rho_A. \tag{3}$$

Analogously, in d-dimensional systems of N noninteracting fermions constrained in a finite volume, the entanglement entropy of a subsystem A shows multiplicative logarithmic corrections to the leading power-law behavior. Indeed it grows asymptotically as [18]

$$S_A^{(\alpha)} \sim N^{(d-1)/d} \ln N. \tag{4}$$

The logarithm of the large-N asymptotic behavior can be related to the logarithmic area-law violation (1) of lattice free fermions, by considering the thermodynamic limit $N, L \to \infty$ keeping the particle density $\rho = N/L^d$ fixed [18]. The leading large-N asymptotic behavior, including its coefficient, can be computed exploiting the

so-called Widom conjecture [11, 14, 16, 18, 19]. However, this approach does not provide information on the next-to-leading terms. These have been conjectured to be logarithmically suppressed with respect to the leading term [18], as in the case of 1D Fermi gases [20, 21] where there are alternative and more powerful approaches to compute the asymptotic behavior of the entanglement entropy, based on the Fisher-Hartwig conjecture [22, 23] and generalizations [24].

In this paper we further investigate this issue. We consider Fermi gases of N particles in a finite L^d volume at equilibrium at $T = 0$, i.e. in their ground state, and compute the first few terms of the asymptotic large-N behaviors of entanglement entropies and particle fluctuations of subsystems with some convenient geometries, which allow us to significantly extend their computation. For example, the half-space vN entanglement entropy of a system of size L^d turns out to asymptotically increase as (setting $L = 1$)

$$S^{(1)}_{\rm HS} = aN^{(d-1)/d}\left[\ln N + a_0 + O\left(N^{-1/d}\right)\right]. \quad (5)$$

We exactly compute the constants a and a_0 for 2D and 3D, for both periodic boundary conditions (PBC) and open (hard-wall) boundary conditions (OBC). The calculation of coefficient a confirms the results already obtained using the Widom conjecture, while that of the constant a_0 provides new information. Moreover, we investigate the successive terms of the expansion which are generally suppressed by powers of $1/N$, and show peculiar oscillations.

Beside the ground-state properties, we consider the nonequilibrium dynamics of Fermi gases after dropping the hard walls of the trap, which allows the gas to expand freely. The free expansion of gases after the drop of the trap is routinely exploited in experiments to infer the properties of the initial quantum state of the particles within the trap [3], by observing the interference patterns of absorption images in the large-time ballistic regime. The quantum dynamics of freely expanding fermionic systems has been much investigated, see e.g. Refs. [3, 25–38], considering also particle systems constrained into lattice structures. In particular, Ref. [38] reports an experimental investigation of the trasport properties during the expansion of fermionic atoms in optical lattices.

Beside being of phenomenological interest, a Fermi gas released from a trap is one of the simplest examples of nonequilibrium unitary evolution, which may provide interesting general information on the nonequilibrium entanglement properties. We are interested in the time dependence of extended observables around the original hard-wall trap, such as entanglement entropies and particle fluctuations associated with finite space regions, during the nonequilibrium dynamics after the drop of the trap. This issue was already studied in 1D Fermi gases [36], finding a logarithmic small-time behavior, $S^{(1)} \approx (1/3)\ln(1/t)$, for the vN entanglement entropy of intervals in proximity to the initial trap, and the relation

$$S^{(1)} \approx \frac{\pi^2}{3} V^{(2)} \quad (6)$$

with the particle variance $V^{(2)}$. These results resemble equilibrium behaviors [20, 39, 40] where the leading logarithms are essentially determined by the corresponding conformal field theory with central charge $c = 1$. We show that analogous relations hold in the nonequilibrium dynamics of higher-dimensional Fermi gas released from hard-wall traps. In the large-N regime we exactly determine the small-t behavior of the entanglement entropy of spatial subsystems A in proximity of the original trap. We find that the relation (6) still holds, and that its asymptotic small-t behavior,

$$S^{(1)}_A(t) \sim t^{1-d}\ln(1/t), \quad (7)$$

is characterized by a multiplicative logarithmic correction to the leading power law.

The paper is organized as follows. In Sec. II we report the many-body wave function describing the ground state of N-particle Fermi gases in cubic-like hard-wall traps, and their free expansion after dropping the trap; moreover we define the extended observables that we consider. In Sec. III we compute the asymptotic large-N behavior of the entanglement entropies and particle fluctuations of strip-like subsystems, which allow us to exactly compute the leading and next-to-leading terms and investigate the power-law suppressed (oscillating) corrections. In Sec. IV we consider Fermi gases in a disk, to investigate the dependence of the large-N asymptotic behavior on the system's shape. Section V is devoted to the study of the entanglement properties of the nonequilibrium dynamics of d-dimensional noninteracting Fermi gases released from a trap; in particular, we determine its small-t and large-t asymptotic behaviors for subsystems corresponding to the original trap. Finally, in Sec. VI we summarize our main results and draw our conclusions.

II. MANY-BODY WAVE FUNCTIONS AND EXTENDED OBSERVABLES

A. Fermi gas within hard walls

We consider a d-dimensional gas of N spinless noninteracting fermionic particles of mass m, confined within a limited space region by a hard-wall trap. For simplicity, we mostly consider cubic-like traps of size L, and place the origin of the axes at the center of the trap, so that the allowed region for the particles is

$$T = [-L/2, L/2]^d. \quad (8)$$

In the following we set $\hbar = 1$ and $m = 1$.

The ground-state wave function is

$$\Psi(\mathbf{x}_1, ..., \mathbf{x}_N) = \frac{1}{\sqrt{N!}}\det[\psi_n(\mathbf{x}_m)], \quad (9)$$

where ψ_n are the lowest N eigensolutions of the free one-particle Schrödinger equation with the appropriate boundary conditions. For example, assuming open (hard-wall) boundary conditions, the eigensolutions can be written as a product of eigenfunctions of the corresponding 1D Schrödinger problem, i.e.

$$\psi_n(\mathbf{x}) \equiv \psi_{n_1,n_2,...,n_d}(\mathbf{x}) = \prod_{i=1}^{d} \varphi_{n_i}(x_i), \qquad (10)$$

$$E_{n_1,n_2,...,n_d} = \sum_{i=1}^{d} e_{n_i}, \qquad (11)$$

where the subscript n_i labels the eigenfunctions along the d directions, which satisfy $\varphi_n(-L/2) = \varphi_n(L/2) = 0$, thus

$$\varphi_n(x) = \frac{1}{\sqrt{L/2}} \sin\left(n\pi \frac{x + L/2}{L}\right), \quad e_n = \frac{\pi^2}{2L^2} n^2, \qquad (12)$$

for $n = 1, 2, ...$

The one-particle correlation function reads

$$C(\mathbf{x}, \mathbf{y}) \equiv \langle c^\dagger(\mathbf{x}) c(\mathbf{y}) \rangle = \sum_{n=1}^{N} \psi_n(\mathbf{x})^* \psi_n(\mathbf{y}), \qquad (13)$$

where $c(\mathbf{x})$ is the fermionic annihilation operator. The particle density $\rho(\mathbf{x}) = \langle n(\mathbf{x}) \rangle$, where $n(\mathbf{x}) \equiv c^\dagger(\mathbf{x}) c(\mathbf{x})$, and the connected density-density correlation $G_n(\mathbf{x}, \mathbf{y}) \equiv \langle n(\mathbf{x}) n(\mathbf{y}) \rangle_{\mathbf{c}}$ can be easily derived from the two-point function; for example $\rho(\mathbf{x}) = \sum_{n=1}^{N} |\psi_n(\mathbf{x})|^2$.

Other interesting observables are related to the particle-number distribution over a spatial region A, which is described by the expectation value and correlations of the particle-number operator $\hat{N}_A \equiv \int_A d^d x\, n(\mathbf{x})$. A more powerful characterization of the particle distribution is achieved using its cumulants $V_A^{(m)}$ [41]. In particular, the particle variance reads

$$V_A^{(2)} = \langle \hat{N}_A^2 \rangle - \langle \hat{N}_A \rangle^2. \qquad (14)$$

A measure of the entanglement of the extended region A with the rest of the system is provided by the vN and Rényi entanglement entropies, cf. Eq. (2).

In noninteracting Fermi gases the particle cumulants and the entanglement entropies of a subsystem A can be related to the two-point function C restricted within A [42], which we denote by $C_A(\mathbf{x}, \mathbf{y})$. For example, the particle number and cumulants within A can be derived using the relations $N_A = \mathrm{Tr}\, C_A$ and [43]

$$V_A^{(m)} = (-i\partial_z)^m \mathcal{G}(z, C_A)|_{z=0}, \qquad (15)$$

$$\mathcal{G}(z, \mathbb{X}) = \mathrm{Tr} \ln\left[1 + \left(e^{iz} - 1\right) \mathbb{X}\right]. \qquad (16)$$

The computation of the particle cumulants and entanglement entropies in Fermi gases of N particles is much simplified by introducing the $N \times N$ overlap matrix $\mathbb{A}$,

$$\mathbb{A}_{nm} = \int_A d^d x\, \psi_n^*(\mathbf{x}) \psi_m(\mathbf{x}), \qquad n, m = 1, ..., N, \quad (17)$$

where the integration is over the spatial region A, and involves the lowest N energy levels. Indeed, exploiting the relation

$$\mathrm{Tr}\, \mathbb{A}^k = \mathrm{Tr}\, C_A^k \qquad (18)$$

for any k, one can compute the particle cumulants and the entanglement entropies from the eigenvalues a_n of the overlap matrix [20, 21, 40, 44]. For example

$$S_A^{(\alpha)} = \frac{1}{1-\alpha} \sum_{n=1}^{N} \ln\left[{a_n}^\alpha + (1 - a_n)^\alpha\right]. \qquad (19)$$

In the limit $\alpha \to 1$ we recover the formula for the vN definition.

For noninteracting fermions, one can write down a formal expansion of the entanglement entropies of bipartitions in terms of the even cumulants $V_A^{(2k)}$ of the particle-number distribution. Indeed, the Rényi entropies can be written as [45, 46]

$$S_A^{(\alpha)} = \sum_{k=1}^{\infty} s_k^{(\alpha)} V_A^{(2k)}, \qquad (20)$$

$$s_k^{(\alpha)} = \frac{(-1)^k (2\pi)^{2k} 2\zeta[-2k, (1+\alpha)/2]}{[(\alpha - 1)\alpha^{2k}(2k)!]},$$

where ζ is the generalized Riemann zeta function. The expansion (20) gets effectively truncated in the large-N limit. Indeed, in Eq. (20) the leading $O(N^{(d-1)/d} \ln N)$ asymptotic behavior of $S_A^{(\alpha)}$ arises from $V_A^{(2)}$ only, because the leading order of each cumulant $V^{(m)}$ with $m > 2$ vanishes for any subsystem A (including disjoint ones) in any dimension [40], and also in the presence of an external space-dependent confining potential [44]. This implies the general asymptotic relation [40]

$$S_A^{(\alpha)} / V_A^{(2)} = (1 + \alpha^{-1}) \pi^2/6 + o(1). \qquad (21)$$

B. Fermi gas released from the hard-wall trap

We also consider the nonequilibrium evolution of a Fermi gas initially in its ground state within the hard-wall trap (8), after the instantaneous drop of the trap. This is described by the time-dependent wave function

$$\Phi(\mathbf{x}_1, ..., \mathbf{x}_N; t) = \frac{1}{\sqrt{N!}} \det[\phi_n(\mathbf{x}_m, t)] \qquad (22)$$

where $\phi_n(\mathbf{x}, t)$ are the one-particle wave functions with initial condition $\phi_n(\mathbf{x}, 0) = \psi_n(\mathbf{x})$, corresponding to the lowest N states of the one-particle Hamiltonian at $t = 0$. They can be written using the free propagator $\mathcal{P}$ as

$$\phi_n(\mathbf{x}, t) = \int_T d^d y\, \mathcal{P}(\mathbf{x}, t; \mathbf{y}, 0) \psi_n(\mathbf{y}), \qquad (23)$$

$$\mathcal{P}(\mathbf{x}, t; \mathbf{y}, 0) = \prod_{i=1}^{d} P(x_i, t; y_i, 0),$$

$$P(x, t; y, 0) = \frac{1}{\sqrt{i2\pi t}} \exp\left[\frac{i(x-y)^2}{2t}\right].$$

FIG. 1: (Color online) A schematic representation of the subsystems (shadowed) considered in 2D: (a) a strip centered within the system; (b) a strip starting at one edge. Of course, in the case of PBC they are equivalent.

The equal-time observables can again be written in terms of the one-particle wave functions, essentially by replacing the equilibrium wave functions $\psi_n(\mathbf{x})$ with the time-dependent wave function $\phi_n(\mathbf{x},t)$. For example, the equal-time one-particle and connected density-density correlation functions read

$$C(\mathbf{x},\mathbf{y},t) = \sum_{n=1}^{N} \phi_n(\mathbf{x},t)^* \phi_n(\mathbf{y},t), \tag{24}$$

$$G_n(\mathbf{x},\mathbf{y},t) = -|C(\mathbf{x},\mathbf{y},t)|^2 + \delta(\mathbf{x}-\mathbf{y})C(\mathbf{x},\mathbf{y},t). \tag{25}$$

The particle cumulants and the entanglement entropies of a subsystem A can be again related to the two-point function C restricted within A [47]. One can also define a time-dependent overlap matrix [36]

$$\mathbb{A}_{nm}(t) = \int_A d^d x\, \phi_n^*(\mathbf{x},t)\phi_m(\mathbf{x},t), \qquad n,m = 1,...,N, \tag{26}$$

where the integration is over the spatial region A, and involves the time evolutions $\phi_n(\mathbf{x},t)$ of the lowest N energy states of the one-particle Schrödinger problem at $t=0$. The time-dependent particle fluctuations within A and the bipartite entanglement entropies can be again computed form the time-dependent eigenvalues of $\mathbb{A}$, using formulas analogous to those at equilibrium [36]. In particular, also Eq. (20) holds during the time evolution.

III. ENTANGLEMENT ENTROPY OF STRIP-LIKE SUBSYSTEMS IN 2D AND 3D

A. Overlap matrix for strip-like subsystems

We consider Fermi gases constrained within the trap region (8) with open (hard-wall) boundary conditions (OBC) and periodic boundary conditions (PBC). The leading large-N behavior (4) of the entanglement entropy of any connected subsystem has been computed by applying the Widom conjecture to evaluate the asymptotic behavior of the formal expressions derived from the overlap matrix. However, this approach does not provide any information on the next-to-leading terms.

We now extend these calculations for some convenient strip-like geometries

$$A = \mathcal{I} \times [-L/2, L/2]^{d-1}, \tag{27}$$

$$\mathcal{I} = [-\delta L/2, \delta L/2], \qquad 0 < \delta < 1, \tag{28}$$

see Fig. 1a. This choice of subsystems significantly simplifies the computations, allowing us to exactly derive the leading and next-to-leading terms of the large-N expansion, and to identify the power law of the corrections.

For our purpose, we exploit the fact that the corresponding overlap matrix (17) is a block diagonal matrix. Indeed, relabeling the indexes n,m of the $N\times N$ overlap matrix as $n_1,...,n_d$ and $m_1,...,m_d$, and using Eq. (10), we can write the half-space overlap matrix as

$$\mathbb{A}_{n_1,...,n_d;m_1,...,m_d} = \mathbb{E}_{n_1 m_1} \prod_{i=2}^{d} \delta_{n_i m_i}, \tag{29}$$

$$\mathbb{E}_{nm} = \int_{\mathcal{I}} dx\, \varphi_n(x)\varphi_m(x), \tag{30}$$

φ_n are the 1D eigenfunctions on the interval $\mathcal{I}$ (for example those reported in Eq. (12) for OBC), the indexes $n_1,...,n_d$ correspond to the lowest N states according to Eq. (11).

B. Leading and next-to-leading terms in 2D systems

1. *Periodic boundary conditions*

Let us first consider a 2D system with PBC. The corresponding one-particle eigenspectrum is given by Eqs. (10) and (11) with

$$\varphi_n(x) = \frac{1}{\sqrt{L}} e^{i2\pi n(x+L/2)/L}, \quad e_n = \frac{2\pi^2}{L^2} n^2, \tag{31}$$

for $n \in \mathbb{Z}$. We construct the ground state of a Fermi gas by filling all states with

$$n_1^2 + n_2^2 \le n_f^2, \qquad n_i \in \mathbb{Z}, \tag{32}$$

and n_f is a real number. The number N of particles is a function of n_f, which asymptotically reads $N \approx \pi n_f^2$. In the following we set $L=1$.

Since the overlap matrix (29) is block diagonal, for any integer k we have

$$\mathrm{Tr}\, \mathbb{A}[N(n_f)]^k = \sum_{n_1=-\lfloor n_f \rfloor}^{\lfloor n_f \rfloor} \mathrm{Tr}\, \mathbb{E}(2\lfloor\sqrt{n_f^2 - n_1^2}\rfloor + 1)^k, \tag{33}$$

where $\lfloor x \rfloor$ indicates the largest integer which is smaller than x, and $\mathbb{E}(M)$ is the $M\times M$ overlap matrix (30) constructed using the lowest M 1D states. This also implies analogous exact relations for all observables O_A which are functions of the eigenvalues of the overlap matrix, such as the particle cumulants and the entanglement entropies. Thus,

$$O_A = \sum_{n_1=-\lfloor n_f \rfloor}^{\lfloor n_f \rfloor} \mathcal{O}_{\mathcal{I}} \left(2\lfloor\sqrt{n_f^2 - n_1^2}\rfloor + 1\right), \tag{34}$$

where $\mathcal{O}_{\mathcal{I}}(M)$ is the corresponding quantity for 1D M-particle systems.

In order to derive their large-N asymptotic behaviors, we replace the sum by an integral

$$O_A(N) = \int_{-n_f}^{n_f} dn\, \mathcal{O}_{\mathcal{I}}\left(2\sqrt{n_f^2 - n^2}\right), \tag{35}$$

where n_f is related to the particle number by the asymptotic relation $N = \pi n_f^2$.

Then, we derive the asymptotic large-N behavior of the entanglement entropies and the particle cumulants by inserting the corresponding asymptotic formulas for the 1D quantities, which have been computed using the Fisher-Hartwig conjecture [22, 23] and generalizations [24, 48]. They are [20, 21]

$$\mathcal{S}_{\mathcal{I}}^{(\alpha)}(M) = c_\alpha \left[\ln M + \ln\sin(\pi\delta) + b_\alpha\right] + O(M^{-2/\alpha}), \tag{36}$$

where

$$c_\alpha = \frac{1+\alpha^{-1}}{6}, \tag{37}$$

$$b_\alpha = \ln 2 + \int_0^\infty \frac{dt}{t} \times \tag{38}$$
$$\times\Big[\frac{6}{1-\alpha^{-2}}\Big(\frac{1}{\alpha\sinh t/\alpha} - \frac{1}{\sinh t}\Big)\frac{1}{\sinh t} - e^{-2t}\Big].$$

Concerning the particle cumulants, we have [40]

$$\mathcal{V}_{\mathcal{I}}^{(2)} = \frac{1}{\pi^2}\left[\ln M + \ln\sin(\pi\delta) + v_2\right] + O(M^{-2}), \tag{39}$$

$$\mathcal{V}_{\mathcal{I}}^{(2k)} = v_{2k} + O(M^{-\varepsilon}) \quad \text{for} \;\; k > 1, \tag{40}$$

where

$$v_2 = 1 + \gamma_E + \ln 2, \tag{41}$$

$$v_4 = -0.0185104, \quad v_6 = 0.00808937, \tag{42}$$

etc.... The odd cumulants are suppressed,

$$\mathcal{V}_{\mathcal{I}}^{(2k+1)} = O(M^{-\varepsilon}) \qquad (k \geq 1). \tag{43}$$

The power $\varepsilon > 0$ of the $O(M^{-\varepsilon})$ corrections in the particle cumulants $\mathcal{V}^{(m)}$ with $m \geq 3$ is not known. Numerical results suggest that ε depends on m and that it gets smaller with increasing m. Note that, since the interval $\mathcal{I}$ has two boundaries, analogous formulas hold in the case of OBC, with the only difference that corrections are $O(M^{-1/\alpha})$ in Eq. (36), and $O(M^{-1})$ in Eq. (39).

Inserting the above asymptotic 1D formulas into Eq. (35), we obtain the desired 2D results. The asymptotic behavior of the entanglement entropies turns out to be

$$S_A^{(\alpha)} \approx S_{A,\text{asy}}^{(\alpha)} + O(N^{1/2-\kappa}), \tag{44}$$

$$S_{A,\text{asy}}^{(\alpha)} = \frac{c_\alpha}{\sqrt{\pi}} N^{1/2}\left(\ln N + a_0\right), \tag{45}$$

$$a_0 = 2\ln\sin\pi\delta + 2b_\alpha - \ln\pi + 4\ln 2 - 2. \tag{46}$$

The approximations to derive this asymptotic behavior from Eq. (34) do not affect the leading $O(N^{1/2}\ln N)$ and next-to-leading $O(N^{1/2})$ terms, so that the constants a and a_0 should be considered as exact. Indeed, in the derivation of Eq. (35), replacing the sum with an integral induces $O(N^{-1/2})$ relative errors. The asymptotic 1D behaviors which we inserted in the integrals for the entanglement entropy lead to $O(n^{-2/\alpha})$, thus $O(N^{-1/\alpha})$, corrections; while the fact that we use it also when n is not large should cause $O(N^{-1/2})$ relative corrections (apart from logarithms). This implies that the overall corrections for the entanglement entropies are those reported in Eq. (44) with

$$\kappa = \min[1/2, 1/\alpha]. \tag{47}$$

This will be further checked by numerical calculations below.

For the particle cumulants we obtain

$$V_A^{(2)} = V_{A,\text{asy}}^{(2)} + O(N^0), \tag{48}$$

$$V_{A,\text{asy}}^{(2)} = \frac{1}{\pi^{5/2}} N^{1/2}\left(\ln N + w_0\right), \tag{49}$$

$$w_0 = 2\ln\sin\pi\delta + 2v_2 - \ln\pi + 4\ln 2 - 2, \tag{50}$$

and

$$V_A^{(m)} \approx \frac{2v_m}{\sqrt{\pi}}\, N^{1/2}, \quad m > 2, \tag{51}$$

where v_m are the constants of the leading large-N behavior in 1D, cf. Eqs. (41), (42) and (43). In the case of the particle variance the corrections are expected to be suppressed by $N^{-1/2}$ with respect to the leading term.

Of course, the leading terms with the multiplicative logarithms are in agreement with the results obtained by the Widom conjecture [18, 40].

2. *Open boundary conditions*

In the case of OBC the ground state of the Fermi gas is obtained by filling all states with

$$n_1^2 + n_2^2 \leq n_f^2, \qquad n_i \in \mathbb{N}, \tag{52}$$

where n_f is asymptotically related to the particle number by $N \approx (\pi/4) n_f^2$. We have again the general relations

$$\text{Tr}\,\mathbb{A}[N(n_f)]^k = \sum_{n_1=1}^{\lfloor n_f \rfloor} \text{Tr}\,\mathbb{E}\left(\lfloor\sqrt{n_f^2 - n_1^2}\rfloor\right)^k \tag{53}$$

for any $k \in \mathbb{N}$, between the trace of powers of the corresponding overlap matrix $\mathbb{A}$ and the reduced 1D $\mathbb{E}$, cf. Eq. (29). Then, in the case of the subsystem A, cf. Eq. (27), one can easily check that the same asymptotic behaviors of PBC apply. One should however expect that corrections to the above asymptotic formulas are larger, essentially because the 1D asymptotic behaviors

have larger corrections. Indeed, for the entanglement entropies we expect that they are $O(N^{-\kappa})$ with $\kappa = 1/(2\alpha)$ with respect to the leading term. The particle variance should have $O(N^{-1/2})$ corrections as well.

The above results change if we consider strip-like subsystems which start from the boundary, essentially because the corresponding asymptotic 1D behaviors change [20, 40]. For example, we apply the same approach to the half-space subsystem defined as

$$H = [-L/2, 0] \times [-L/2, L/2]^{d-1}, \tag{54}$$

and shown in Fig. 1b. In this case the corresponding 1D asymptotic large-N behaviors change [20, 40], for example

$$\mathcal{S}^{(\alpha)}_{\mathcal{H}}(M) = \frac{c_\alpha}{2}\left[\ln M + \ln 2 + b_\alpha\right] + O(M^{-1/\alpha}) \tag{55}$$

where $\mathcal{H} = [-L/2, 0]$, essentially because only one boundary separates the two parts. The asymptotic behaviors of the half-space entanglement entropies and particle cumulants are

$$S^{(\alpha)}_H = S^{(\alpha)}_{H,\text{asy}} + O(N^{1/2-1/(2\alpha)}), \tag{56}$$

$$S^{(\alpha)}_{H,\text{asy}} = \frac{c_\alpha}{2\sqrt{\pi}} N^{1/2}(\ln N + a_0), \tag{57}$$

$$a_0 = 2b_\alpha - \ln\pi + 6\ln 2 - 2, \tag{58}$$

and

$$V^{(2)}_H = V^{(2)}_{H,\text{asy}} + O(N^0) \tag{59}$$

$$V^{(2)}_{H,\text{asy}} = \frac{1}{2\pi^{5/2}} N^{1/2}(\ln N + w_0), \tag{60}$$

$$w_0 = 2v_2 - \ln\pi + 6\ln 2 - 2, \tag{61}$$

$$V^{(m)}_H \approx \frac{v_m}{\sqrt{\pi}} N^{1/2}, \quad m > 2. \tag{62}$$

C. Leading and next-to-leading terms of the entanglement entropy in 3D systems

The above calculations can be easily extended to strip-like subsystems in higher-dimensional systems. We construct the ground state 3D Fermi gases with PBC, by filling all states with

$$n_1^2 + n_2^2 + n_3^2 \le n_f^2, \qquad n_i \in \mathbb{Z}, \tag{63}$$

and the number N of particles is a function of n_f, asymptotically $N = 4\pi n_f^3/3$. Exploiting again the block structure of the corresponding overlap matrix (29), we can write any observable O_A, defined in terms of the eigenvalues of A, as

$$O_A = 4\int_0^{n_f} dn_1 \int_0^{\sqrt{n_f^2 - n_1^2}} dn_2\, \mathcal{O}_{\mathcal{I}}\left(2\sqrt{n_f^2 - n_1^2 - n_2^2}\right). \tag{64}$$

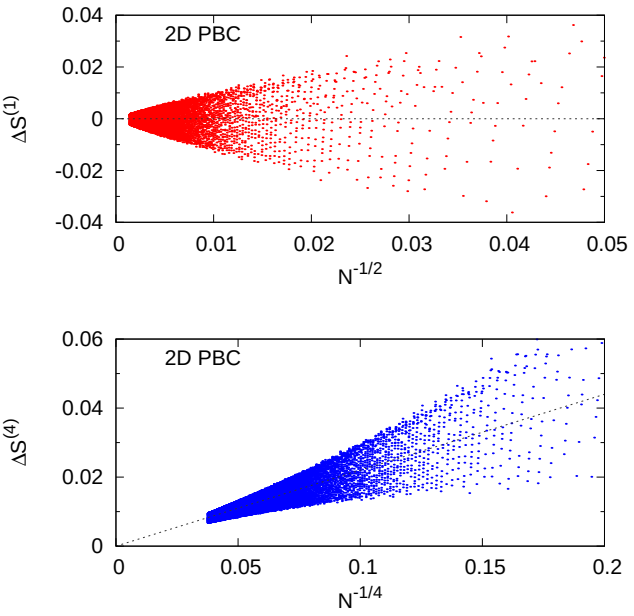

FIG. 2: (Color online) We plot the subtracted half-space vN and $\alpha = 4$ Rényi entropies defined in Eq. (70), for a 2D Fermi gas with PBC. The powers of N reported in abscissa are the expected power laws of the large-N scaling corrections. The lines are drawn to guide the eyes.

Again, by replacing the large-N behavior $\mathcal{S}_{\mathcal{I}}$ of the 1D, we obtain

$$S^{(\alpha)}_A = S^{(\alpha)}_{A,\text{asy}} + O(N^{2/3-\kappa}), \tag{65}$$

$$S^{(\alpha)}_{A,\text{asy}} = \frac{\pi^{1/3} c_\alpha}{2^{4/3}3^{1/3}} N^{2/3}\left(\ln N + a_0\right), \tag{66}$$

$$a_0 = 3\ln\sin\pi\delta + 3b_\alpha - \ln\pi + \ln 6 - 3/2.$$

The same asymptotic behaviors apply to the case of OBC. An analysis of the errors induced by the approximations indicate that the corrections are suppressed by $O(N^{-\kappa})$, with $\kappa = \min[1/3, 2/(3\alpha)]$ for PBC and $\kappa = 1/(3\alpha)$ for OBC, with respect to the leading term. Analogous results can be obtained for the particle fluctuations.

In the case of OBC we also consider the half-space region (54), obtaining

$$S^{(\alpha)}_H = S^{(\alpha)}_{H,\text{asy}} + O(N^{2/3-1/(3\alpha)}), \tag{67}$$

$$S^{(\alpha)}_{H,\text{asy}} = \frac{\pi^{1/3} c_\alpha}{2^{7/3}3^{1/3}} N^{2/3}(\ln N + a_0), \tag{68}$$

$$a_0 = 3b_\alpha - \ln\pi + \ln 24 - 3/2. \tag{69}$$

D. Oscillating corrections to the asymptotic behavior

We now present finite-N numerical results obtained by explicitly computing the eigenvalues of the overlap

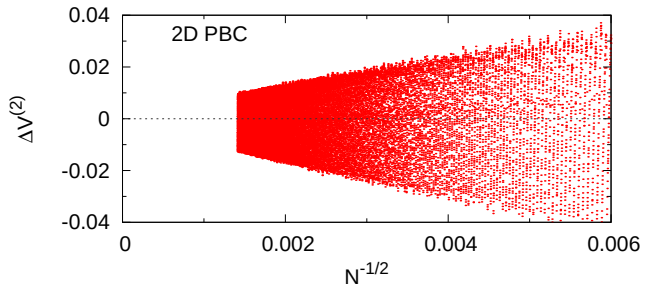

FIG. 3: (Color online) We plot the subtracted half-space particle variance defined as in Eq. (70), for a 2D Fermi gas with PBC.

matrix (17) and plugging them into the formula (19) [20, 40]. We compare their behavior with increasing N, up to $N = 5\times10^5$ and $N = 3\times10^7$ for 2D and 3D, respectively, with the exact asymptotic behaviors derived above, and study the deviations, for which we previously argued the power-law suppression. In particular, we show that such corrections are characterized by peculiar oscillations.

For this purpose, we show data for the half-space entanglement entropies and particle variance after subtracting the asymptotic behaviors computed in the previous subsections, i.e for the quantities

$$\Delta O \equiv N^{-(d-1)/d}\,[O_{\rm HS}(N) - O_{\rm HS,asy}]\,, \qquad (70)$$

where the asymptotic formula for $S^{(\alpha)}$ and $V^{(2)}$ are reported in Eqs. (45), (49), (57), (60), (66), and (68), for 2D and 3D, with PBC and OBC. The data for OBC refer to the half-space region defined in Eq. (54).

Figs. 2 and 3 report results for the vN and Rényi entanglement entropies and the particle variance, respectively, for the half space of 2D systems with PBC. The data support the asymptotic behaviors obtained previously. In particular, the subtracted quantities (70) appear to vanish with increasing N with the expected power laws (possibly multiplied by a logarithmic factor), i.e. $N^{-\kappa}$ with $\kappa = \min[1/2, 1/\alpha]$ for the entanglement entropies and $N^{-1/2}$ for the particle variance. Note however that such corrections are characterized by wide oscillations. Analogous results are obtained for the half-space entanglement entropies in the case of OBC, as shown by Figs. 4 and 5, respectively in 2D and 3D systems.

The oscillations of 2D systems exhibit a distinctive structure, and are essentially related to the way the Fermi sphere is filled as we add more particles to the system. In particular, it is interesting to note that an oscillation of the vN entanglement entropy corresponds to $n_f \to n_f+1$, cf. Eq. (32). This is shown by the data of Fig. 6 for the vN entanglement entropy of 2D systems with PBC.

For any integer n_f, the smallest block contributing to the calculation is of size $n_{\rm min} = 1$, and is obtained by setting $n_1 = \pm n_f$ in the right hand side of Eq. (34). Note that the size of the second smallest block, $n^{(2)}_{\rm min}$,

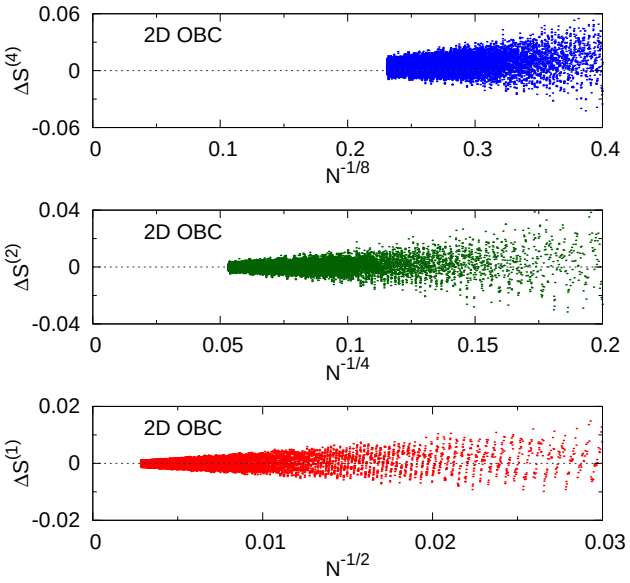

FIG. 4: (Color online) We plot the subtracted half-space vN and $\alpha = 2, 4$ Rényi entropies defined in Eq. (70), for a 2D Fermi gas with OBC. The powers of N reported in abscissa are the expected power laws of the large-N scaling corrections.

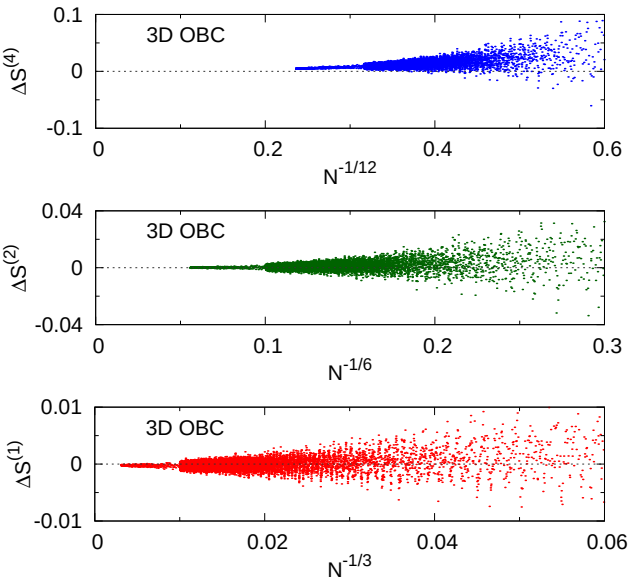

FIG. 5: (Color online) We plot the subtracted half-space vN and $\alpha = 2, 4$ Rényi entropies defined in Eq. (70), for a 3D Fermi gas with OBC. The powers of N reported in abscissa are the expected power laws of the large-N scaling corrections.

corresponding to $n_1 = \pm(n_f - 1)$, grows with n_f as

$$n^{(2)}_{\rm min}(n_f) = 2\lfloor\sqrt{2n_f - 1}\rfloor \longrightarrow 2\lfloor\sqrt{2n_f}\rfloor \sim N^{1/4}. \qquad (71)$$

Therefore, except for the blocks of size one, which contribute with a constant, the smallest blocks are asymptotically large, thus justifying the use of asymptotic formulas in Eq. (34). However, if we release the require-

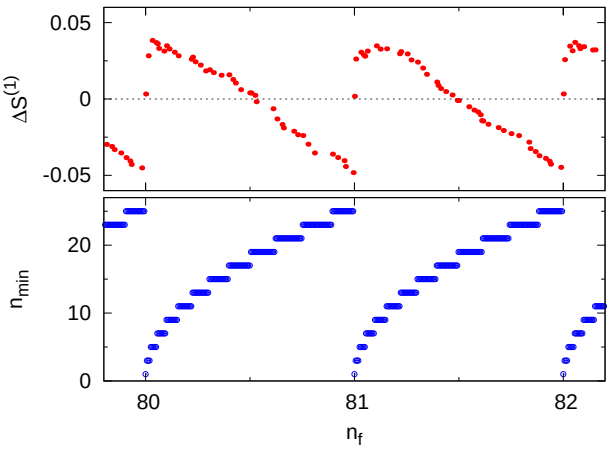

FIG. 6: (Color online) Top: we plot the quantity (70) for the half-space vN entanglement entropy of a 2D Fermi gas with PBC, versus n_f. The oscillating corrections show a periodic behavior with respect to n_f, with period $\Delta n_f = 1$. Bottom: for comparison, we also plot the size $n_{\min}$ of the smallest 1D block intervening in the calculation, which presents similar oscillations.

ment that n_f be an integer, $n_{\min}$ is in general greater than one, and Eq. (71) provides an upper bound to it. Following the quantity $n_{\min}$ from an integer n_f to n_f+1, $n_{\min}$ starts by taking unit value, then monotonically increases up to $n^{(2)}_{\min}(n_f+1)$, finally dropping again to one (cf. bottom panel of Fig. 6). A comparison of data for $n_{\min}(N)$ with the oscillating corrections to the asymptotic behavior of the half-space vN entanglement entropy is shown in Fig. 6. The connection between the two quantities is evident, and can be heuristically explained by considering the "specific entropy" carried by each 1D block that contributes to the sum Eq. (34). According to Eq. (36), we can define the specific entropy of a block $s(n) = S_{1D}(n)/n \sim (\ln n)/n$, which is a function with an absolute maximum for $n \approx 0.3$. The specific entropy is then monotonically decreasing for any integer n. Small blocks add few particles but lots of entropy, and thus give a positive correction over the asymptotic formula (44), which in the subtracted data plotted in Fig. 6 approximately correspond to the line $y = 0$. On the other hand, larger blocks add many particles but relatively little entropy, and hence explain the descending part of the oscillation. This reasoning only makes use of the geometric characteristics of the Fermi sphere and of the leading behaviour of the entanglement entropies for 1D gases, which is shared among all the quantities we study in this paper. Therefore the same explanation of the oscillations apply to the particle variance as well.

In dimension higher than two, a similar analysis of the oscillations would lead to a decomposition in terms of superpositions of many 1D blocks at once, thus explaining the more complex structure of higher order corrections to the entanglement entropy shown in Fig. 5. Note also that in the case of the Rényi entropies ($\alpha \geq 2$) and higher cumulants, as well as for strips of width other than the half space, some oscillations already appear in the correction to the asymptotic 1D behavior [21, 40], and may result in further contributions and modulations of the oscillatory corrections in 2D.

IV. FERMI GAS ON A DISK

In order to understand how extended observables may depend on the shape of the hard-wall trap, we consider a Fermi gas in a disk D of unit radius $R = 1$ with hard-wall boundary conditions. Its many-body wave function is still given by Eq. (9) with one-particle eigenfunctions satisfing the boundary condition $\psi_k(R, \theta) = 0$ in spherical coordinates. The one-particle normalized eigenspectrum is given by

$$\psi_{nl}(r,\theta) = \frac{1}{\sqrt{\pi} J_{|l|+1}(k_{nl})} J_{|l|}(k_{nl} r) e^{il\theta}, \tag{72}$$

where $l \in \mathbb{Z}$ and $n \in \mathbb{N}$, $k_{nl} > 0$ is the n^{th} zero (excluding the origin) of the Bessel function $J_{|l|}$, and the energy levels are $e_{nl} = k^2_{nl}/2$.

Let us consider a subsystem A given by a disk of radius $r < R = 1$. In order to derive the leading large-N behavior of their entanglement entropy, we use the large-area asymptotic formula [18]

$$S^{(\alpha)}_A \approx \frac{1+\alpha^{-1}}{6\sqrt{\pi}} \rho^{1/2} \mathcal{A} \ln \mathcal{A}, \tag{73}$$

where $\mathcal{A}$ is the area separating A from the rest, and ρ is the particle density. This result was derived [18] by turning the large-N behavior of $\ell_1 \times \ell_2$ subsystems in square L^2 systems into the large-area behavior in the thermodynamic limit keeping $\rho = N/V$ fixed. Note that since we are now considering a different geometry we cannot straighforwardly use the large-N results of rectangular subsystems in square systems. However, we expect that, in the thermodynamic limit keeping $\rho \equiv N/V$ fixed, the coefficient of the logarithmic correction to the area law depends only on the particle density. In other words, when it is expressed in terms of the local particle density, it is expected to be independent of the system shape. Then we turn the large-area asymptotic behavior (73) into a large-N asymptotic behavior assuming that the limits can be interchanged. In the case at hand, replacing $\mathcal{A} = 2\pi r$ and $N = \pi R^2 \rho$ into Eq. (73), we obtain

$$S^{(1)}(r) \approx \frac{r}{3} N^{1/2} \ln N \tag{74}$$

for the vN entropy.

We check this asymptotic behavior by finite-N computations based on the overlap matrix (17) using the one-particle eigenspectrum (72). Some numerical results are reported in Fig. 7 for $r = 1/4$ and $r = 1/2$. They clearly support Eq. (74), with the same pattern of corrections

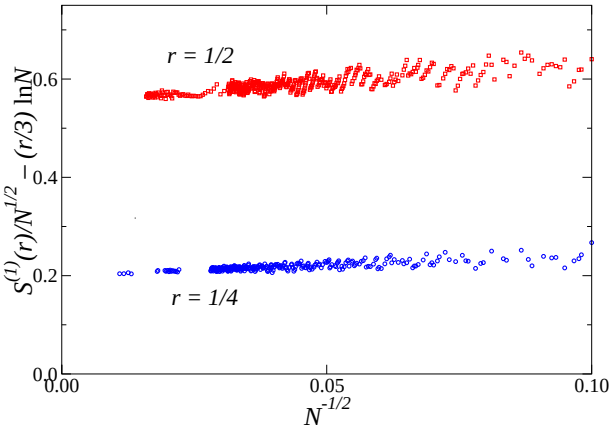

FIG. 7: (Color online) The vN entanglement entropy of disks of radius $r = 1/4$ and $r = 1/2$ with respect to the rest, in Fermi gases constrained within a disk of of size $R = 1$. We plot $N^{-1/2}S^{(1)}(r) - \frac{r}{3}\ln N$ vs $N^{-1/2}$.

found in the systems considered in the previous section, i.e.

$$S^{(1)}(r) = \frac{r}{3}N^{1/2}(\ln N + a_0) + O(N^0), \qquad (75)$$

and show again oscillations, which appear to increase with increasing r.

V. FERMI GASES RELEASED FROM A TRAP

In this section we consider the free expansion of the Fermi gas after the instantaneous drop of the hard-wall trap $T = [-L/2, L/2]^d$, described by the many-body wave function reported in Sec. II B. In the following we set $L/2 = 1$; the dependence on the trap size can be easily recovered by a dimensional analysis. We determine the time evolution of entanglement entropies and particle fluctuations for a large number of particles.

A. The large-N limit

The equal-time two-point function can be written as

$$C(\mathbf{x},\mathbf{y},t) = \qquad (76)$$
$$\sum_{k=1}^{N}\int_T d^d z_1\, d^d z_2\, \mathcal{P}(\mathbf{x},t;\mathbf{z}_1,0)\mathcal{P}(\mathbf{y},t;\mathbf{z}_2,0)\,\phi_k(\mathbf{z}_1)\phi_k(\mathbf{z}_2)$$

where $T = [-1,1]^d$. The large-N limit of the equal-time two-point function can be obtained using the completeness relation [49]

$$\sum_{k=1}^{\infty}\phi_k(\mathbf{x})\phi_k(\mathbf{y}) = \delta(\mathbf{x}-\mathbf{y}) \qquad (77)$$

of the spectrum of the one-particle Hamiltonian at $t = 0$. We obtain the large-N limit

$$C_\infty(\mathbf{x},\mathbf{y},t) = \prod_{i=1}^{d}\frac{\sin[(y_i-x_i)/t]}{\pi(y_i-x_i)}\, e^{i(x_i^2-y_i^2)/(2t)}. \qquad (78)$$

This implies that the large-N limit of the time evolution of the particle density is simply

$$\rho_\infty(\mathbf{x},t) = C_\infty(\mathbf{x},\mathbf{x},t) = \frac{1}{(\pi t)^d}, \qquad (79)$$

which is independent of the position. Of course, this regime is approached nonuniformly with respect to the spatial coordinate, but it is rapidly reached around the central region of the size of the original trap, i.e. $|\mathbf{x}| \lesssim 1$. The density-density correlation function can be obtained using Eq. (25).

In order to compute quantities that depend only on the eigenvalues of the restriction C_A of C within an extended region A, such as the entanglement entropies, we can further simplify Eq. (78) by dropping the phases, retaining only

$$\mathbb{C}_A(\mathbf{x},\mathbf{y},t) = \prod_{i=1}^{d}\mathbb{Y}(x_i,y_i,t), \qquad (80)$$

$$\mathbb{Y}(x,y,t) = \frac{\sin[(y-x)/t]}{\pi(y-x)}. \qquad (81)$$

Let us now consider an extended cubic-like subsystem

$$A = [-s,s]^d, \qquad (82)$$

with s of the size of the original trap. The large-N particle number $n_\infty(t)$ and cumulants $V_\infty^{(m)}(t)$ of the subsystem A can be written in terms of the 1D traces

$$\mathcal{T}_k \equiv \mathrm{Tr}_{[-s,s]}\,\mathbb{Y}^k, \qquad (83)$$

so that $\mathrm{Tr}\,\mathbb{C}_A^k = \mathcal{T}_k^d$. Indeed we have

$$n_\infty(t) = \mathcal{T}_1^d = \left(\frac{2s}{\pi t}\right)^d, \qquad (84)$$

and

$$\begin{aligned} V_\infty^{(2)}(t) &= \mathrm{Tr}\,\mathbb{C}_A(1-\mathbb{C}_A) = \mathcal{T}_1^d - \mathcal{T}_2^d, \qquad (85)\\ V_\infty^{(3)}(t) &= \mathrm{Tr}\,(\mathbb{C}_A - 3\mathbb{C}_A^2 + 2\mathbb{C}_A^3) = \mathcal{T}_1^d - 3\mathcal{T}_2^d + 2\mathcal{T}_3^d,\\ V_\infty^{(4)}(t) &= \mathrm{Tr}[\mathbb{C}_A - 7\mathbb{C}_A^2 + 12\mathbb{C}_A^3 - 6\mathbb{C}_A^4] =\\ &= \mathcal{T}_1^d - 7\mathcal{T}_2^d + 12\mathcal{T}_3^d - 6\mathcal{T}_4^d, \end{aligned}$$

etc. In particular, for the space region $A = [-1,1]^d$, i.e. $s = 1$, which coincides with the original trap, we obtain

$$\mathcal{T}_1 = \frac{2}{\pi t}, \qquad (86)$$

$$\mathcal{T}_2 = \int_{-1}^{1} dx\, dy\, \mathbb{Y}(x,y)^2 = \qquad (87)$$
$$= \frac{4\mathrm{Si}(4/t) - t[1+\gamma_E + \ln(4/t) - \cos(4/t) - \mathrm{Ci}(4/t)]}{\pi^2 t}$$

where Ci and Si are the cosine and sine integral functions. The small-t asymptotic expansion of the particle variance can be easily derived, obtaining

$$V^{(2)}_{\infty,\mathrm{asy}}(t) = \frac{2^{d-1}d}{\pi^{d+1}} t^{1-d} \left[\ln(1/t) + 1 + \gamma_E + 2\ln 2\right] + O\left[t^{2-d}\ln^2(1/t)\right]. \quad (88)$$

Note that the above calculations can be easily extended to anisotropic rectangular-like traps and/or subsystems, although they become more cumbersome.

B. The small-t behavior of particle cumulants and bipartite entanglement entropies

The Eqs. (85) allow us to relate the small-t asymptotic behaviors of the particle cumulants to those obtained in 1D Fermi gases released from a 1D trap $[-1,1]$ and associated with the interval $[-s,s]$, which are [36]

$$\mathcal{V}^{(2)}_{\mathrm{asy}}(t) \approx \frac{1}{\pi^2}\left[\ln(1/t) + \ln 2s + v_2\right], \quad (89)$$

$$\mathcal{V}^{(2k+1)}_{\mathrm{asy}}(t) \approx 0 \qquad (k \geq 1), \quad (90)$$

$$\mathcal{V}^{(2k)}_{\mathrm{asy}}(t) \approx v_{2k} \qquad (k \geq 2), \quad (91)$$

where v_2, v_4, etc. are the same constants appearing in in Eqs. (41) and (42). Indeed, these asymptotic expressions allow us to derive the small-t behaviors of $\mathcal{T}_k$, cf. Eq. (83). By inserting them in Eq. (85), we obtain the d-dimensional asymptotic relation

$$V^{(m)}_{\infty,\mathrm{asy}}(t) = d\left(\frac{2s}{\pi t}\right)^{d-1} \times \mathcal{V}^{(m)}_{\mathrm{asy}}(t). \quad (92)$$

Corrections to this asymptotic behaviors are suppressed by powers of t with respect to the leading term (with possible multiplicative logarithms). In the case of the particle variance the asymptotic behavior (92) coincides with Eq. (88). The comparison with the exact large-N limit $V^{(2)}_{\infty}(t)$, see Fig. 8, shows that for 2D systems Eq. (92) provides a good approximation when $t \lesssim 0.2$.

Therefore, Eq. (92) shows that, like 1D systems [36], only the particle variance has a multiplicative logarithmic correction to the leading power law in the small-t limit, behaving as $V^{(2)}_{\infty}(t) \sim t^{1-d}\ln(1/t)$, while higher even cumulants behave simply as $V^{(2k)} \sim t^{1-d}$, and odd cumulants are relatively suppressed.

In order to derive the small-t asymptotic behaviors of the entanglement entropies, we may use their relation (20) with the particle cumulants. Since only the particle variance has the leading multiplicative logarithm, we obtain the asymptotic small-t relation

$$\frac{S^{(\alpha)}_{\infty}(t)}{V^{(2)}_{\infty}(t)} \approx \pi^2 c_\alpha, \quad (93)$$

where corrections are only logarithmically suppressed.

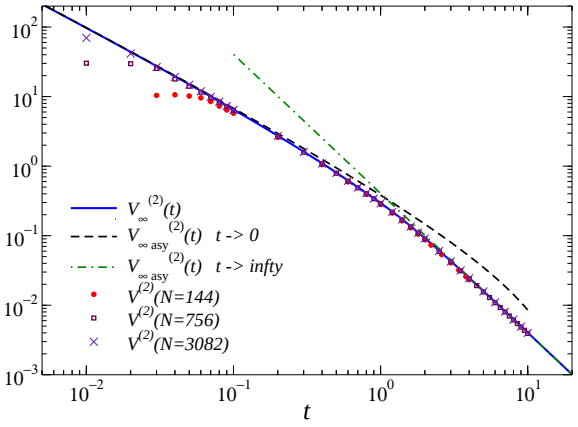

FIG. 8: (Color online) For 2D Fermi gases released by a hard-wall trap $[-1,1]^2$ and a spatial region corresponding to the initial trap, we compare the large-N limit $V^{(2)}_{\infty}(t)$ of the particle variance, obtained from Eqs. (85), (86), (87), with its small-t and large-t asymptotic behaviors, Eqs. (92) and (98) respectively. Moreover, we also show finite-N data which approach the large-N results, nonuniformly with decreasing t.

It is worth mentioning that the same result can also be obtained following the procedure employed in Ref. 36 (see its Sec. IIIB), based on a discretization of the two-point function (81), which maps it to a lattice free-fermion model without boundary, at equilibrium in the thermodynamic limit and with a cubic Fermi surface with $k_F \sim 1/t$. Then, the asymptotic small-t behavior of the entanglement entropy can be evaluated using the Widom conjecture [19], using e.g. the formulas of Ref. [40].

Actually, we can also determine the next-to-leading corrections of the entanglement entropies, by noting that the $O(t^{1-d})$ asymptotic behavior of d-dimensional cumulants is just obtained by multiplying the same factor times the 1D results, cf. Eq. (92). Thus, using Eq. (20), we conjecture that the same result extends to the entanglement entropies, i.e.

$$S^{(\alpha)}_{\infty,\mathrm{asy}}(t) \approx d\left(\frac{2s}{\pi t}\right)^{d-1} \times \mathcal{S}^{(\alpha)}(t) \quad (94)$$

where $\mathcal{S}^{(\alpha)}$ is the asymptotic small-t behavior of 1D systems for the interval $[-s,s]$, i.e. [36]

$$\mathcal{S}^{(\alpha)}(t) = c_\alpha\left[\ln(1/t) + \ln 2s + b_\alpha\right] \quad (95)$$

where c_α and b_α are given in Eqs. (37) and (38). In the small-t regime corrections to Eq. (94) are expected to be relatively suppressed by powers of t.

C. The large-time behavior of entanglement entropies and particle fluctuations

We now compute the large-t behaviors of particle fluctuations and entanglement entropies of a space region $[-s,s]^d$. They can be inferred by looking at the behavior

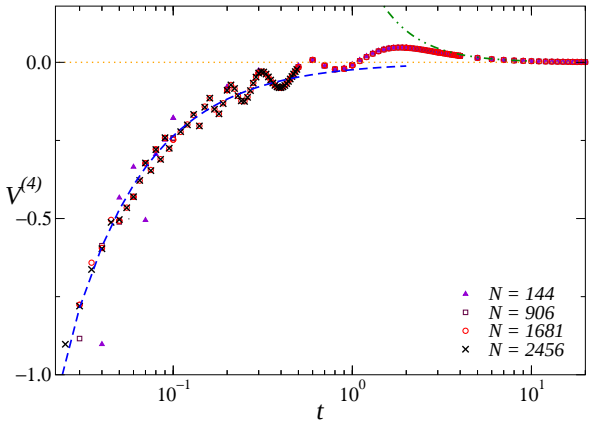

FIG. 9: (Color online) Finite-N results for the quartic cumulant $V^{(4)}$, compared with the large-N results in the small-t regime (dashed line), cf. Eq. (92), and in the large-t regime (dot-dashed line), cf. Eq. (98).

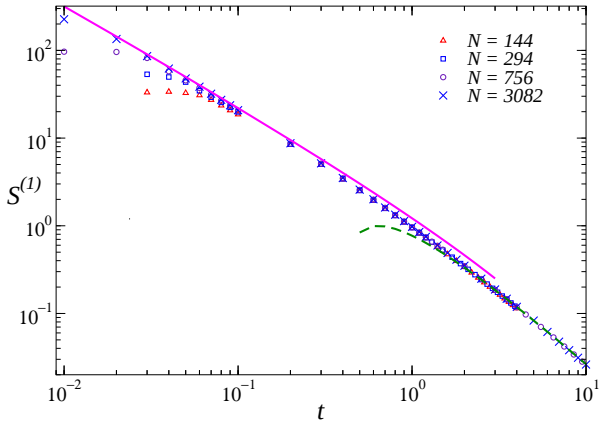

FIG. 10: (Color online) For 2D Fermi gases released by a hard-wall trap $[-1,1]^2$ and the vN entanglement entropy of a spatial region corresponding to the initial trap, we compare finite-N data with the analytical large-N results in the small-t regime (full line), cf. Eq. (94), and in the large-t regime (dashed line), cf. Eq. (99).

of the eigenvalues of the overlap matrix, observing that only one eigenvalue dominates at large time. Indeed, using Eq. (18) and the large-time behavior of $\mathbb{C}_A$, we have

$$\mathrm{Tr}\,\mathbb{A}^k = \mathrm{Tr}\,\mathbb{C}_A^k \sim \left(\frac{2s}{\pi t}\right)^{dk} \tag{96}$$

for any integer k. This implies that the large-t regime of the overlap matrix is characterized by only one nonzero eigenvalue a_1 for any N, given by

$$a_1 \approx \left(\frac{2s}{\pi t}\right)^{d}. \tag{97}$$

The other eigenvalues get rapidly suppressed in the large-t limit.

The largest eigenvalue a_1 determines the asymptotic large-t behaviors of the particle number, particle fluctuations and entanglement entropies:

$$n_A(t) \approx V_A^{(m)} \approx a_1 \quad \text{for any} \;\; m, \tag{98}$$

$$S_A^{(\alpha)} \approx \frac{\alpha}{\alpha-1} a_1, \quad S_A^{(1)} \approx a_1(1-\ln a_1). \tag{99}$$

As shown in Fig. 8, in 2D systems the large-t behavior (98) provides a good approximation of the exact large-N limit (85) of the particle variance for $t \gtrsim 2$.

D. Convergence to the large-N limit

We want to check the actual convergence of the particle fluctuations and entanglement entropies of systems with N particles to the large-N behaviors derived in the preceding subsections, which is generally expected to be chacterized by asymptotic $O(N^{-1/d})$ corrections. For this purpose, we compute them at finite particle number N using the overlap matrix, see Sec. II. We numerically compute its eigenvalues at fixed t, and then obtain the particle cumulants and the entanglement entropies, see Ref. [36] for more details.

We report results for 2D Fermi gases, and subsystems corresponding to the initial square trap. In Fig. 8 we show data for the particle variance. They approach the large-N limit analytically evaluated using Eqs. (85), (86) and (87), although nonuniformly with decreasing t. Fig. 9 shows analogous data for the quartic cumulant $V^{(4)}$, which is characterized by an undulatory large-N limit. In Fig. 10 we show results for the vN entanglement entropy: again the data approach a large-N limit, which is well approximated by the large-N analytical formulas in the small-t and large-t regime, cf. Eq. (94) and (99), for $t \lesssim 0.2$ and $t \gtrsim 2$ respectively. The large-N convergence is more clearly demonstrated in Fig. 11, where we show data of the particle number and particle variance versus $N^{-1/2}$ for some small and fixed values of t. Analogous results are shown in Fig. 12 for the vN entanglement entropy.

As expected the convergence to the large-N limit at fixed t is characterized by leading $O(N^{-1/2})$ corrections, but it does not appear uniform when $t \to 0$. This may suggest some other nontrivial scaling behaviors at small t, which get hidden (pushed toward the $t = 0$ axis) by the large-N limit keeping t fixed, as found in 1D systems [36]. This point may deserve further investigation, but we have not pursued it.

VI. CONCLUSIONS

We study the quantum correlations of 2D and 3D Fermi gases, as described by extended observables such as entanglement entropies and particle fluctuations associated with finite space regions. We mainly consider two

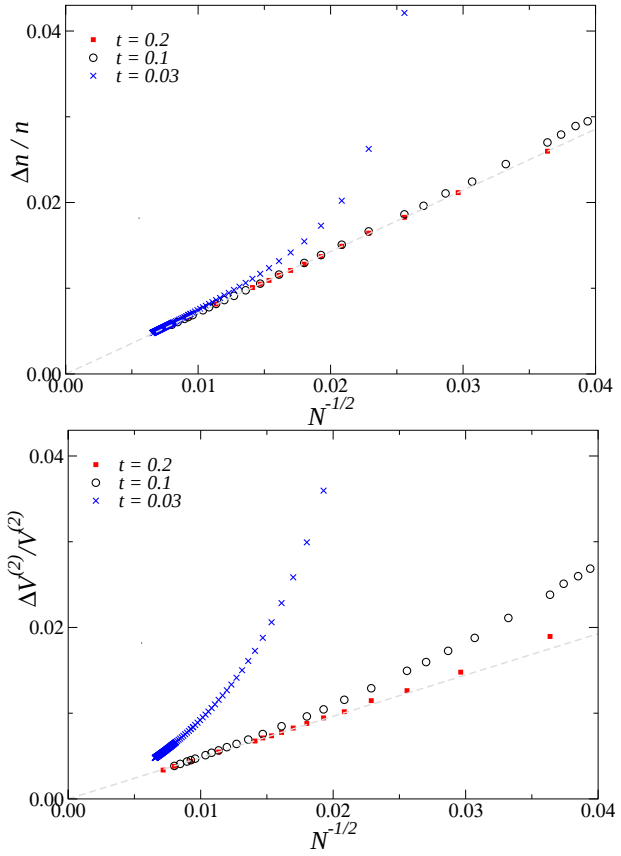

FIG. 11: (Color online) In order to show the convergence to the large-N limit of the particle number $n(t)$ and variance $V^{(2)}(t)$ of the space region $A = T = [-1,1]^2$, we plot the relative differences $\Delta n(t)/n_\infty(t)$ and $\Delta V^{(2)}(t)/V^{(2)}_\infty(t)$, where $\Delta n(t) = n_\infty(t) - n(t;N)$ and $\Delta V^{(2)}(t) = V^{(2)}_\infty(t) - V^{(2)}(t;N)$.

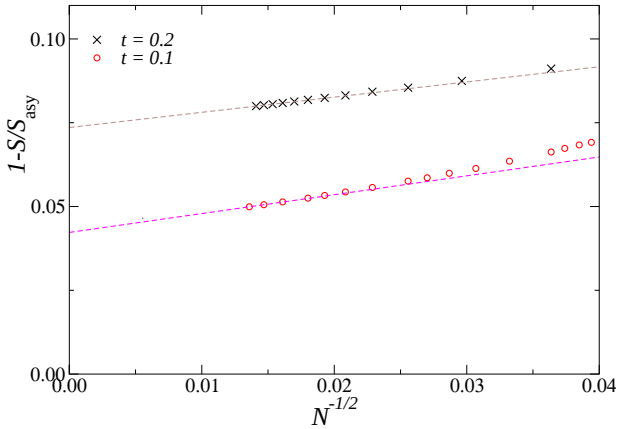

FIG. 12: (Color online) Data for the vN entanglement entropy of the space region $[-1,1]^2$ corresponding to the initial trap, at $t = 0.1$ and $t = 0.2$, and several values of N. We plot $1 - S^{(1)}(t)/S^{(1)}_{\infty,\rm asy}$ where $S^{(1)}_{\infty,\rm asy}$ is the asymptotic (nonexact) formula (94). The dashed lines are linear extrapolations of the data for the largest values of N. The extrapolated nonzero values are consistent with the expected $O(t)$ corrections to the leading small-t terms (94).

physical situations. The Fermi gas of N particles is confined within a limited space region by a hard-wall trap and is at equilibrium at $T = 0$, i.e. in its ground state. Then we consider its nonequilibrium unitary dynamics after the Fermi gas is released from the trap, due to an instantaneous dropping of the trap. This is one of the simplest examples of nonequilibrium unitary evolution of many-body systems, which may provide interesting general information on the nonequilibrium entanglement properties, also in dimensions larger than one.

Within the ground state of 2D and 3D Fermi gases in cubic-shaped hard-wall traps, we compute the leading and next-to-leading terms of the asymptotic large-N behaviors of entanglement entropies and particle fluctuations of strip-like subsystems. Their simple geometry allows us to significantly extend earlier calculations based on the so-called Widom conjecture, which were limited to the leading term without providing any information on the subleading terms. For example, in the case of a 3D Fermi gas in a cubic box of size $L = 1$ with hard-wall boundary conditions, the half-space vN entanglement entropy, i.e. associated with the space region $[0, L/2] \times L^2$ (see Fig. 1b), behaves as

$$S^{(1)}_H = \frac{\pi^{1/3}}{2^{7/3}3^{4/3}} N^{2/3} \Big[\ln N + 3b_1 + + \ln(24/\pi) - 3/2 + O(N^{-1/3}) \Big] \qquad (100)$$

where the constant b_1 comes from 1D calculations, cf. Eq. (38), and the suppressed corrections are also characterized by peculiar oscillations, discussed in Sec. III D.

We then consider the nonequilibrium unitary evolution of the Fermi gases after instantaneously dropping the hard-wall trap. We investigate the entanglement properties during the expansion, by computing the vN and Rényi entanglement entropies and the particle cumulants of extended space regions in proximity to the initial trap. Like 1D systems [36], in the large-N limit the equal-time two-point function assumes a relatively simple form, given by Eq. (78), which can be further simplified when considering only the eigenvalues of its space restrictions, effectively reducing it to

$$\mathbb{C}(\mathbf{x},\mathbf{y},t) = \prod_i \frac{\sin[(y_i - x_i)/t]}{\pi(y_i - x_i)}. \qquad (101)$$

This allows us to derive some exact results on the particle cumulants, in particular the particle variance, and the small-t asymptotic behavior of the entanglement entropies of space regions in proximity to the original trap. For example, the vN entanglement entropy of the subsystem $[-1,1]^d$, coinciding with the original trap, behaves as (we set $L = 2$ for the size of the trap, cf. Eq. (8), which implies that time is measured in units of $m(L/2)^2/\hbar$)

$$S^{(1)}_\infty(t) = \frac{2^{d-1} d}{3\pi^{d-1}} t^{1-d} \left[\ln(1/t) + \ln 2 + b_1 + O(t) \right], \qquad (102)$$

at small t, and

$$S_\infty^{(1)}(t) \approx d \left(\frac{2}{\pi t}\right)^d \ln t \tag{103}$$

in the large-t limit.

These results are obtained in the large-N limit keeping t fixed, which turns out not to be uniform when $t \to 0$. However, the analysis of numerical results at finite N, obtained using the method based on the overlap matrix, shows that the approach to the large-N limit is quite rapid, for example in 2D a few hundred particles are already sufficient to show the main features of the large-N time dependence.

We also note that, analogously to 1D systems, also in higher dimensions the small-t dependence of the entanglement entropy and particle fluctuations show some analogies with the asymptotic behaviors at equilibrium. For example, in the small-t regime $S_A^{(1)} \approx (\pi^2/3)V_A^{(2)}$, which has been shown to be valid for the ground state of a large number of noninteracting Fermi particles, in any dimensions and for any subsystems, in homogeneous and inhomogeneous conditions [40, 44]. Moreover, the small-t dependence (102) shows multiplicative logarithmic corrections to the leading power law, similarly to the area-law violations (1).

The analogies between the small-t and equilibrium asymptotic behaviors are essentially connected with the form of the equal-time two-point function during the free expansion from a hard-wall trap. Indeed, as noted in Sec. V B and also discussed in Ref. [44] within 1D systems, $\mathbb{C}(\mathbf{x}, \mathbf{y}, t)$ corresponds to an appropriate continuum limit of the two-point function of a lattice free-fermion model without boundaries, at equilibrium in the thermodynamic limit and with a cubic Fermi surface with $k_F \sim 1/t$.

An important remark is that some features of the nonequilibrium free expansion from hard-wall traps are closely related to the initial (almost homogenous) conditions. For example, Fermi gases starting from harmonic traps, realized using external space-dependent potentials, show other peculiar nonequilibrium entanglement properties [36], such as that the entanglement entropies can be expressed as a global time-dependent rescaling of the space dependence of the initial equilibrium entanglement entropy, in any dimension.

Within particle systems released from hard-wall traps, further interesting issues may concern the universality of the results reported in this paper, in particular the universality of the small-time asymptotic behaviors of the entanglement entropies and particle fluctuations, whether they are shared with other many-body systems, and their stability against particle interactions.

[1] E.A. Cornell and C.E. Wieman, Rev. Mod. Phys. 74, 875 (2002).
[2] N. Ketterle, Rev. Mod. Phys. 74, 1131 (2002).
[3] I. Bloch, J. Dalibard, and W. Zwerger, Rev. Mod. Phys. 80, 885 (2008).
[4] A. Polkovnikov, K. Sengupta, A. Silva, and M. Vengalattore, Rev. Mod. Phys. 83, 863 (2011).
[5] Entanglement entropy in extended systems, P. Calabrese, J. Cardy, and B. Doyon Eds., J. Phys. A 42, 500301 (2009).
[6] L. Amico, R. Fazio, A. Osterloh, and V. Vedral, Rev. Mod. Phys. 80, 517 (2008).
[7] J. Eisert, M. Cramer, and M.B. Plenio, Rev. Mod. Phys. 82, 277 (2010).
[8] P. Calabrese and J. Cardy, J. Phys. A 42, 504005 (2009).
[9] M.M. Wolf, F. Verstraete, M. B. Hastings, and J. I. Cirac, Phys. Rev. Lett. 100, 070502 (2008).
[10] M.M. Wolf, Phys. Rev. Lett. 96, 010404 (2006).
[11] D. Gioev and I. Klich, Phys. Rev. Lett. 96, 100503 (2006).
[12] T. Barthel, M.-C. Chung, and U. Schollwöck, Phys. Rev. A 74, 022329 (2006).
[13] W. Li, L. Ding, R. Yu, T. Roscilde, and S. Haas, Phys. Rev. B 74, 073103 (2006).
[14] R. Helling, H. Leschke, and W. Spitzer, Int. Math. Res. Not. 2011, 1451 (2011).
[15] L. Ding, N. Bray-Ali, R. Yu, and S. Haas, Phys. Rev. Lett. 100, 215701 (2008).
[16] A. Sobolev, Functional Anal. App. 44, 313 (2010); arXiv:1004.2576.
[17] B. Swingle, Phys. Rev. Lett. 105, 050502 (2010).
[18] P. Calabrese, M. Mintchev, and E. Vicari, Europhys. Lett. 97, 20009 (2012).
[19] H. Widom, Oper. Th.: Adv. Appl. 4, 477 (1982).
[20] P. Calabrese, M. Mintchev, and E. Vicari, Phys. Rev. Lett. 107, 020601 (2011).
[21] P. Calabrese, M. Mintchev, and E. Vicari, J. Stat. Mech. P09028 (2011).
[22] M.E. Fisher and R.E. Hartwig, Adv. Chem. Phys. 15, 333 (1968).
[23] E.L. Basor and K.E. Morrison, Lin. Alg. Appl. 202, 129 (1994).
[24] P. Deift, A. Its, and I. Krasovsky, Ann. Math. 174, 1243 (2011).
[25] A. del Campo, G. Garcá-Calderón, and J.G. Muga, Phys. Rep. 476, 1 (2009).
[26] P. Öhberg and L. Santos, Phys. Rev. Lett. 89, 240402 (2002).
[27] P. Pedri, L. Santos, P. Öhberg, and S. Stringari, Phys. Rev. A 68, 043601 (2003).
[28] A. Minguzzi and D.M. Gangardt, Phys. Rev. Lett. 94, 240404 (2005).
[29] M. Rigol and A. Muramatsu, Phys. Rev. Lett. 94, 240403 (2005).
[30] A. del Campo and J.G. Muga, Europhys. Lett. 74, 965 (2006).
[31] D.M. Gangardt and M. Pustilnik, Phys. Rev. A 77, 041604 (2008).
[32] F. Gerbier, S. Trotzky, S. Fölling, U. Schnorrberger, J.D. Thompson, A. Widera, I. Bloch, L. Pollet, M. Troyer, B. Capogrosso-Sansone, N.V. Prokof'ev, and

B.V. Svistunov, Phys. Rev. Lett. 101, 155303 (2008).
[33] F. Heidrich-Meisner, M. Rigol, A. Muramatsu, A.E. Feiguin, and E. Dagotto, Phys. Rev. A 78, 013620 (2008).
[34] F. Heidrich-Meisner, S.R. Manmana, M. Rigol, A. Muramatsu, A.E. Feiguin, and E. Dagotto, Phys. Rev. A 80, 041603(R) (2009).
[35] S. Langer, M.J.A. Schuetz, I.P. McCulloch, U. Schollwöck, and F. Heidrich-Meisner, Phys. Rev. A 85, 043618 (2012).
[36] E. Vicari, Phys. Rev. A 85, 062324 (2012).
[37] C.J. Bolech, F. Heidrich-Meisner, S. Langer, I.P. McCulloch, G. Orso, and M. Rigol, Phys. Rev. Lett. 109, 110602 (2012).
[38] U. Schneider, L. Hackermüller, J.P. Ronzheimer, S. Will, S. Braun, T. Best, I. Bloch, E. Demler, S. Mandt, D. Rasch, and A. Rosch, Nature Phys. 8, 213 (2012).
[39] P. Calabrese and J. Cardy, J. Stat. Mech. P06002 (2004).
[40] P. Calabrese, M. Mintchev, and E. Vicari, Europhys. Lett. 98, 20003 (2012).
[41] E. Lukacs, *Characteristic functions* (C. Griffin, London 1970).
[42] I. Peschel, J. Phys. A 36, L203 (2003).
[43] H.F. Song, S. Rachel, C. Flindt, I. Klich, N. Laflorencie, and K. Le Hur, Phys. Rev. B 85, 035409 (2012).
[44] E. Vicari, Phys. Rev. A 85, 062104 (2012).
[45] I. Klich and L. Levitov, Phys. Rev. Lett. 102, 100502 (2009).
[46] H.F. Song, C. Flindt, S. Rachel, I. Klich, and K. Le Hur, Phys. Rev. B 83, 161408 (2011).
[47] I. Peschel and V. Eisler, J. Phys. A 42, 504003 (2009).
[48] M. Fagotti and P. Calabrese, J. Stat. Mech. P01017 (2011).
[49] L.D. Landau and L.M. Lifshitz, *Quantum Mechanics Non-Relativistic Theory*, Pergamon Press, 1977.